www.cadanda.com
Computer-Aided Design AND APPLICATIONS

Study of a Point Cloud Segmentation with Part Type Recognition for Tolerance Inspection of Plastic Components via Reverse Engineering

Michele Bici[1], Francesca Campana[2], Stefano Petriaggi[3] and Luca Tito[4]

[1]Dip. di Ing. Meccanica e Aerospaziale, La Sapienza Università di Roma, bici.michele@gmail.com
[2]Dip. di Ing. Meccanica e Aerospaziale, La Sapienza Università di Roma, francesca.campana@uniroma1.it
[3]Divisione Controllo Qualità, ABB SpA – Automation Products Division, Pomezia, stefano.petriaggi@it.abb.com
[4]Divisione Controllo Qualità, ABB SpA – Automation Products Division, Pomezia, luca.tito@it.abb.com

ABSTRACT

This paper presents a point cloud segmentation based on a spatial multiresolution discretisation that is derived from hierarchical space partitioning. Through part type recognition it aims to simplify Computer Aided Tolerance Inspection of electromechanical components avoiding cloud-CAD model registration. A voxel structure subdivides the point cloud. Then, through a suitable surface partitioning, it is linked to component volumes by means of the morphological components of the binary image that is derived from voxel attributes ('true state' if points are included in a specific cluster or 'false state' if they are not). The proposed approach is then applied on a din-rail clip of a breaker, made by injection moulding. This case study points out the suitability of the approach on box-shaped components or with normal protrusions, and its limits concerning the assumptions of the implementation.

Keywords: computer aided tolerance inspection, reverse engineering, segmentation.

1. INTRODUCTION

Electromechanical components made through injection moulding need inspections for die set-up and also for quality control to avoid local and global defects (like surface deflections or flashes) and guarantee the assigned functional tolerances. The adoption of automatic procedures is appreciated to reduce time to market and in particular, reverse engineering techniques are becoming more diffused thanks to the improvements achieved in the field of non-contact measurement systems. Among different non-contact probes suitable for reverse engineering of mechanical components (laser probes, moiré fringe interferometry, structured lighting, etc.) laser scanning is one of the most widespread techniques for industrial on-line control due to its good balance between acquisition time and accuracy [6], [7]. It is faster than Coordinate-Measuring Machines (CMM) allowing to acquire 20,000 points/s with accuracy of 0.025 mm. These characteristics confirm the applicability of laser scanning also for tolerance inspection of plastic components that are manufactured via injection moulding since, in the range of (25, 150) mm, they typically have dimensional tolerance > 0.05 mm.

The automation of tolerance inspection via reverse engineering techniques can be regarded as a general CMM measurement protocol that is enriched with CAD capabilities, like data management and automatic extraction of tolerance specification and solid model reference [2], [4]. It can be summarised according to the general workflow of Fig. 1(a).

Bottlenecks of such implementation are: (a) registration of the point cloud with the CAD model that may ask for expensive fixtures; (b) accuracy of the multiple view recomposition; (c) efficiency of the segmentation algorithms.

From the industrial point of view, they represent time consuming steps since they require manual interactions between CAD model and reverse engineering software. In case of inspections on a large number of electromechanical plastic specimens, as it happens during die set-up, these interactions must be avoided and generally, no specific fixtures are used except a reference table. So, point cloud and CAD model registration becomes less relevant. Moreover the results of the inspection often require the report of many dimensional tolerances, better described as standard 2D technical drawing or datasheet instead

Taylor & Francis

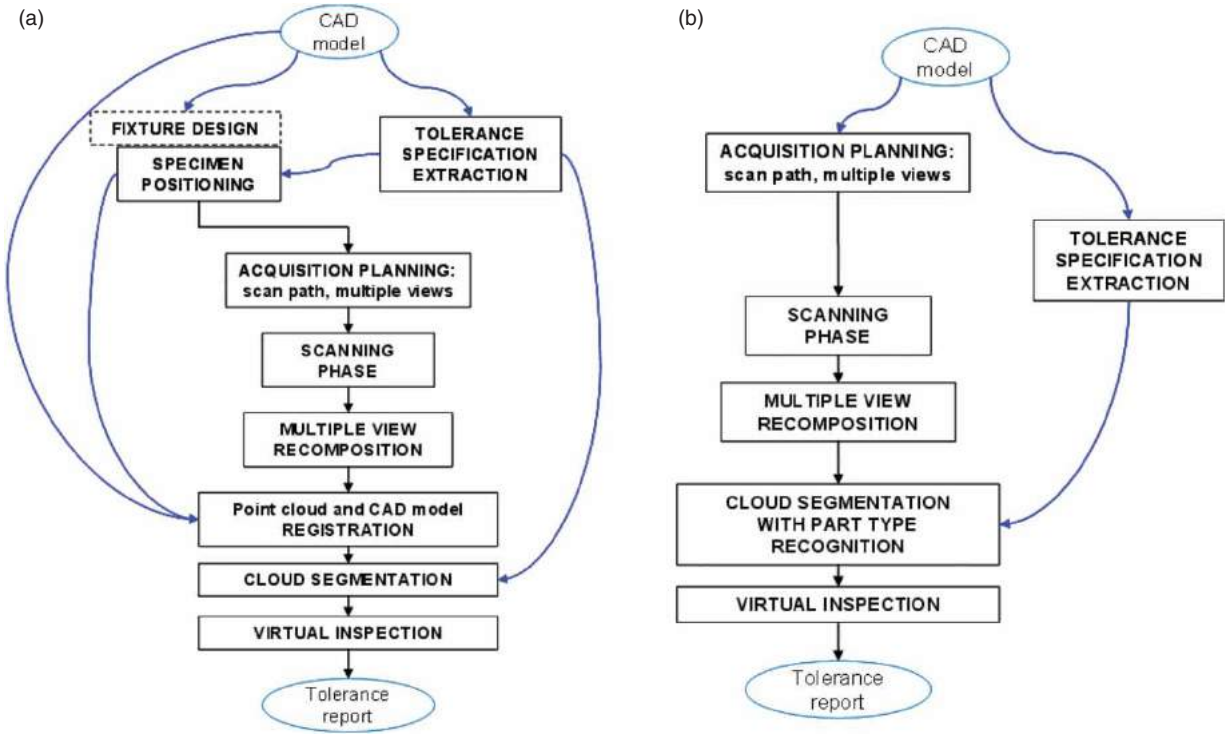

Fig. 1: Computer Aided Inspection: (a) based on CMM measurement protocol; (b) based on part type recognition.

of a deviation distribution on a solid model. These practical needs justify the research of ad hoc procedures able to by-pass the registration phase allowing a virtual inspection that is stand-alone from the CAD model, except for the tolerance specification extraction. This leads to a simplified workflow, shown in Fig. 1(b), where the point cloud and CAD model registration is replaced with a cloud segmentation with part type recognition. The basic idea of this procedure concerns with searching volumes defined by the point cloud surfaces. Doing so a hierarchical tree of features associated with one of the CAD models can be found, so that data to be inspected can be extracted without a registration procedure.

This paper addresses the feasibility of this simplified inspection procedure, referring to tolerance control of plastic components acquired by laser scanning. Starting from the review works of [9] it searches a suitable part type segmentation, to distinguish different volumes, according to the semantic significance requested by the specific application (examples of this derive from the field of image analysis or computer vision). In the specific case of reverse engineering of mechanical parts this segmentation can be related to a problem of feature recognition, [3].

To reach the required automation the paper studies a point cloud segmentation with part type recognition based on a grid method similar to an octree grid derived from hierarchical space partitioning [5]. From this method a 3D voxel structure encompasses the point cloud discerning point presence by the attribute of 'true state' or 'false state' (1 or 0). Merging this information with the surface partition of the cloud it is possible to deduce the link between surfaces and volumes, for example via image analysis techniques.

In the next section the proposed method is explained, then in section 3 it is applied on a test case related to a din-rail clip of a breaker, that was acquired by laser scanning. In section 4 a discussion is presented about the sensitivity of the input parameters, necessary to run the proposed procedure, and, finally, in section 5 main conclusions are outlined.

2. PROPOSED APPROACH

The proposed approach can be divided in two steps. The first one deals with the problem of surface partition, identifying planes and curved surfaces. The second one deals with the part type recognition, finding component volumes associated to the partitioned areas.

Both of them are based on the computation of a 3D structure of voxels that is superimposed on the acquired cloud of points. It is managed as a cubic matrix of $N \times N \times N$ elements associated to the values 1 or 0 ('true' or 'false') depending if they include points of the cloud or not.

The bounding box of the point cloud, $\boldsymbol{P}$, is ideally divided along each of the three reference axes

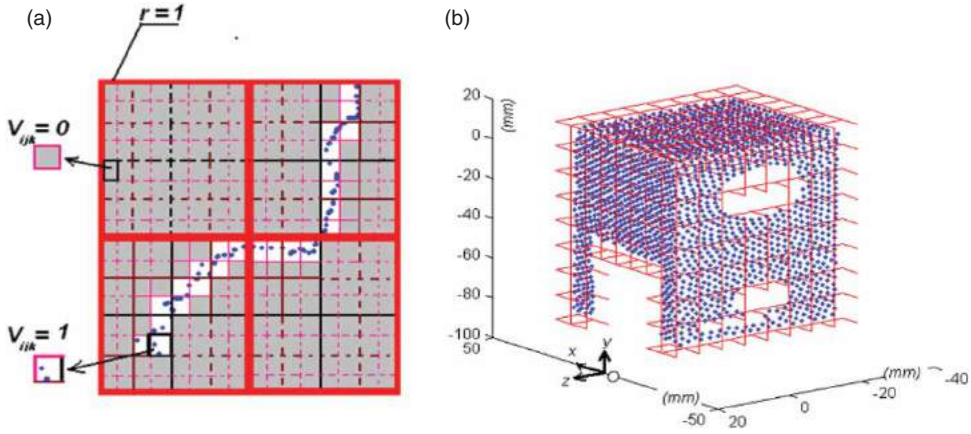

Fig. 2: Structure of voxels: (a) logical scheme for the assignment of V_{ijk}; (b) example of a 3D structure of 'true state' voxels.

according to a step defined as:

$$step_i = \frac{\max(P_i) - \min(P_i)}{k_i} \quad i = x, y, z \tag{2.1}$$

To reduce calculation efforts k_i is recursively replaced up to reach N steps according to a numerical progression, that is usually set as:

$$k_i = 2^r \quad r = 0, ..., \log_2 N \tag{2.2}$$

Doing so matrix values of the 3D structure of voxels, V_{ijk}, are evaluated starting from a cubic volume of 1 *x* 1 *x* 1 that is equivalent to a single large voxel that encompasses the point cloud. Then this initial voxel is split along each reference axis, through the temporary value of $step_i$ defined according to r, that can be seen as a zoom factor. At each iteration, the program verifies what are the temporary voxels without points of the cloud inside, so that all V_{ijk} included within them are set to zero and the local splitting is stopped. On the contrary if points are present it continues looking for new empty, smaller, voxels until the overall N *x* N *x* N matrix is assigned.

Fig. 2(a) gives an example related to an in plane acquisition, assuming $r = 4$ to reach a 16 *x* 16 2D structure. Grey voxels are in 'false state', white ones are in 'true state'. Continuous lines represent temporary voxels analysed updating r, whereas dot lines represent V_{ijk} assigned before the updating (without local splitting). At the end of this process all the V_{ijk} elements in the 'true' state encompass the points, approximating the surface associated to the acquisition as shown in the 3D structure of Fig. 2(b).

Through the computation of a proper adjacency matrix it is possible to keep track of voxel connections differentiating them according to face, edge or vertex connections. This step is preliminary to part type partitioning as follows.

First of all it is necessary the identification of the voxels that include planar surfaces, recognizing plane direction and extension. For each V_{ijk} in the 'true' state a local plane is fit by least square minimisation made through single value decomposition. Then a first partition is obtained analysing the variance of the point distances from the local plane inside the voxel. It has been found that the most populated bin of the variance distribution on the voxels is always the first one. It can be assumed as a threshold to exclude all V_{ijk}, that are filled with non planar regions of the cloud. Fig. 3(a) shows a typical occurrence histogram of the variance while Fig. 3(b). gives an example of the results achieved through this threshold procedure. Doing so voxels with variance values greater than that of the most populated bin are turned off, excluding V_{ijk} with cloud regions which belong to non planar surfaces or small radii (blue points depicted in Fig. 3(b)).

Through this threshold all the voxels that are univocally associated to planes are identified and small radius areas are separated but the information about plane extension, position and associated feature are still missing.

To do so an hybrid region growing – hierarchical clustering procedure has been set up to find groups of V_{ijk} which are both connected and filled with planes of equal direction. The unit vectors associated to the normals of the best-fit planes inside the voxels, $(n_x\ n_y\ n_z)_{ijk}$, are verified to specific unit directions, $(a\ b\ c)$, for example the reference axes, by means of a threshold condition derived from the so-called L_2 orientation norm [9]:

$$L_2 = 1 - (n_x \quad n_y \quad n_z)_{ijk} \cdot (a \quad b \quad c)^T \leq \varepsilon \tag{2.3}$$

This threshold, from now on called 'normal dot product threshold', is verified for each pair of the voxel's adjacency matrix, then this matrix is updated with a code about the effective plane direction of each pair. Through this new adjacency matrix, plane partition is then completed via hierarchical clustering starting from a seed value defined according to the specific directions analysed with eqn. (2.3).

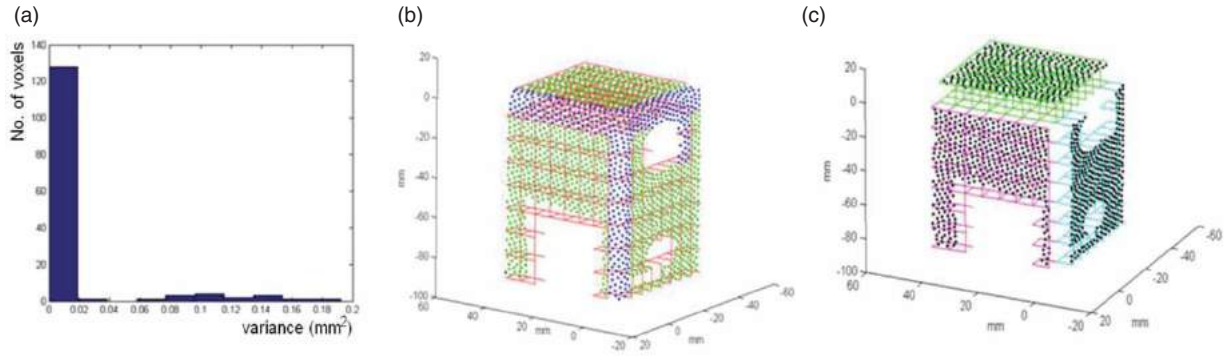

Fig. 3: Plane partition: (a) occurrence histogram of the variance computed from the voxel's best fit planes; (b) example of small radii or non planar region recognition, points in blue; (c) plane partition along the three reference axes.

The specific direction, $(a\ b\ c)$, is taken from a set of unit normals, S, that is defined by means of an iterative procedure inserted inside the clustering phase according to this reasoning. Since eq. (2.3) is checked recursively on each i,j,k when it is found "false", a new direction $(a\ b\ c)_{new} = (n_x\ n_y\ n_z)_{ijk}$ is added to S if:

$$\begin{cases} 1 - (n_x \quad n_y \quad n_z)_{ijk} \cdot (a \quad b \quad c)_0^T > \varepsilon \\ \forall (a \quad b \quad c)_0 \in S \end{cases} \tag{2.4}$$

Doing so at the end of the region growing – hierarchical clustering procedure a plane clustering is done according to every significant directions of the acquired component that are found in S.

The resulting planes are then fitted on the overall points owned by the voxels of each cluster. Typically these planes are the ones inspected for dimensional check and also in this case they are computed by means of a least squares minimisation.

After the plane partition the part recognition starts. It is made for the purpose of associating planes to specific volumes, that can be recognized knowing the tree of the CAD model geometric features. As a first step the procedure is here explained considering only volumes obtained by normal protrusion of planes along the reference axes, but then they represent the large part of features involved in electromechanical components.

This step can be seen as an image analysis based technique and follows the workflow of Fig. 4.

Each plane found through the cluster analysis is a potential start or end plane for a protruded detail of the component. Reading as a binary image the 2D voxel matrix associated to a generic plane of a cluster and comparing it to the binary image of the next sections (that are derived in the same way) a protruded volume exists if the morphological components of these images are comparable. As it is showing through the case study in section 3, the analysis of the boundary traces of each section is made inspecting also if there are some nested profiles inside the holes. This allows to find a structure

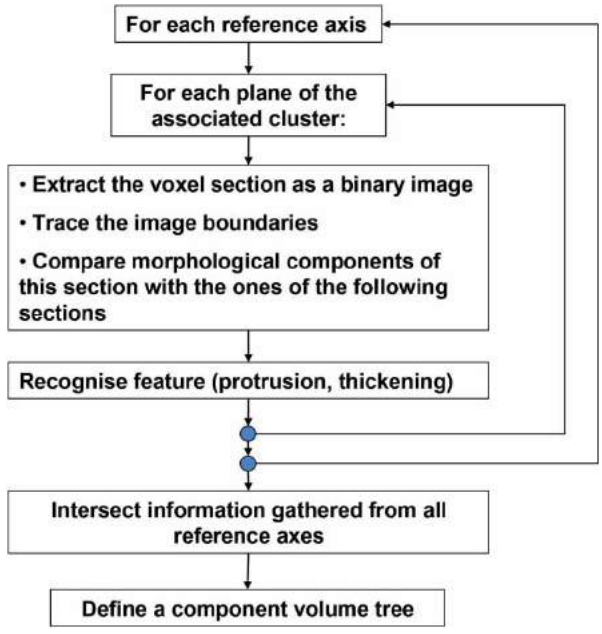

Fig. 4: Logical workflow of the part type recognition associated to CAD operation normal to the reference axes.

of elementary volumes along the reference axis directions, that can be set as equivalent to part of the CAD features involved in the tolerance inspection.

3. CASE STUDY

The proposed approach is here applied on an industrial example concerning with the acquisition of a din-rail clip of a breaker, made of Delrin 100 by injection moulding (Fig. 5).

It was acquired by a Nikon LC15Dx laser scanner, placed on a CMM controller system (3Coord Hera 12.9.7). The laser scanner has a probing error of 0.0025 mm (obtained with test comparable to EN/ISO 10360-2) and can acquire approximately 70,000 points/sec, and 900 points per line. The CMM system

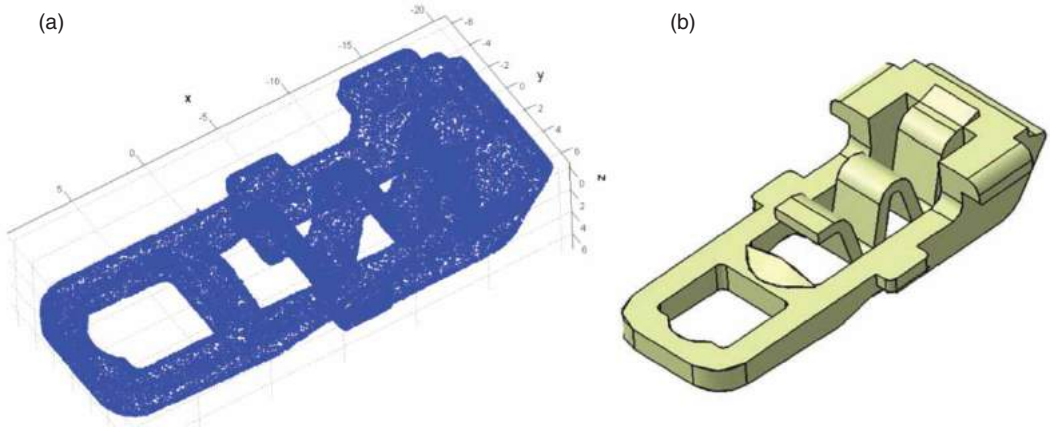

Fig. 5: Din-rail clip: (a) laser scanner acquisition, length unit: mm; (b) solid model.

has a range of accuracy of about $(2, 6) \times 10^{-3}$ mm with a positioning maximum speed of 750 mm/s. By means of this system a cloud of over 6×10^4 points was obtained.

The proposed approach has been applied assuming:

- $N = 32$, that means a zoom factor $r = 5$;
- 20 bins for the variance threshold;
- a normal dot product threshold to search for planes normal to the three reference axes $\geq$ 0.999.

Fig. 6(a) shows the achieved results in terms of final 'true' state voxels. A total amount of 1896 V_{ijk} is equal to "1" ('true state' voxels) while the other 30872 are set to "0"('false state').

Fig. 6(b) shows the result of the preliminary partition made through the voxel's variance threshold. In this case, adopting 20 bins, the variance threshold is equal to 0.0014 mm^2, that corresponds to a standard deviation from the voxels' best fitting plane of $\pm$0.0374 mm. This threshold excludes other 384 voxels, mainly localized on small radius or curved surfaces (blue points in Fig. 6(b)). Finally, Fig. 6(c) shows the clusters obtained through the hybrid region growing – hierarchical clustering procedure applying the normal dot product threshold to search for planes that are normal to the three reference axes.

From these planes the part type recognition can start. To understand the feasibility of this approach, we are now referring to the volume recognition associated to plane clusters normal to the y axis (magenta points of Fig. 6(c)). In this case the surface partition step recognises eight planes. Four of them (the widest) are depicted in the upper part of Fig. 7 as binary images of the voxel sections. In the lower part the results of the boundary tracing is shown in terms of labeled areas.

Through the bonding box of the labelled areas the sequence of filled and empty regions can be localized on the 3D structure of voxels, thus on the point cloud (e.g. three distinct areas are found: blue one is filled, yellow and cyan are empty). These sequences are associated to finite volumes of the component comparing their morphological components with that of the images derived from the neighbouring sections.

In the specific case the bounding box of the blue area of each section has been compared with the neighbouring ones according to: (i) centroid position,

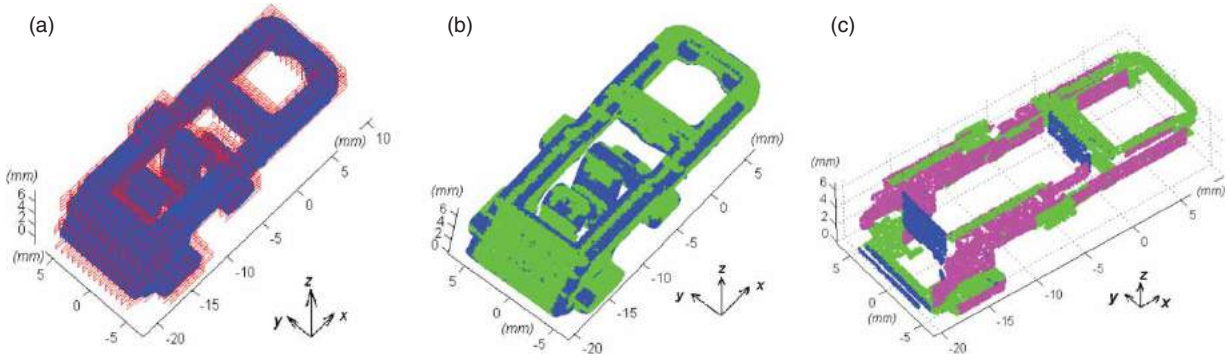

Fig. 6: Din-rail clip: (a) 3D structure of 'true state' voxels; (b) voxel detection with small radii or non planar region, blue points; (c) clusters found for planes perpendicular to the reference axes - blue x axis; magenta y axis; green z axis.

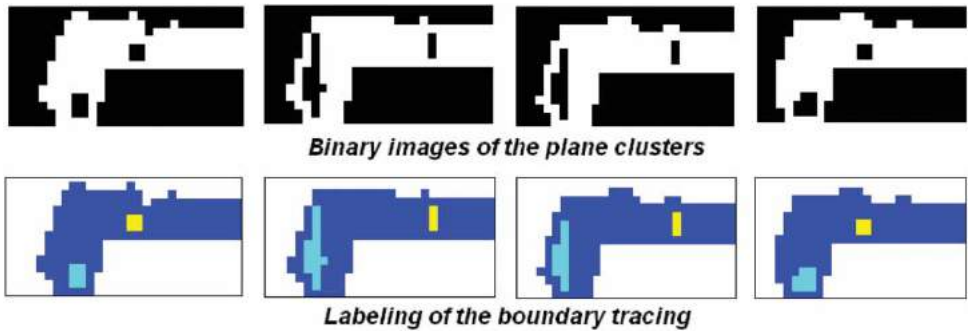

Fig. 7: Part type recognition: binarisation and boundary tracing of four plane sections normal to the *y* axis.

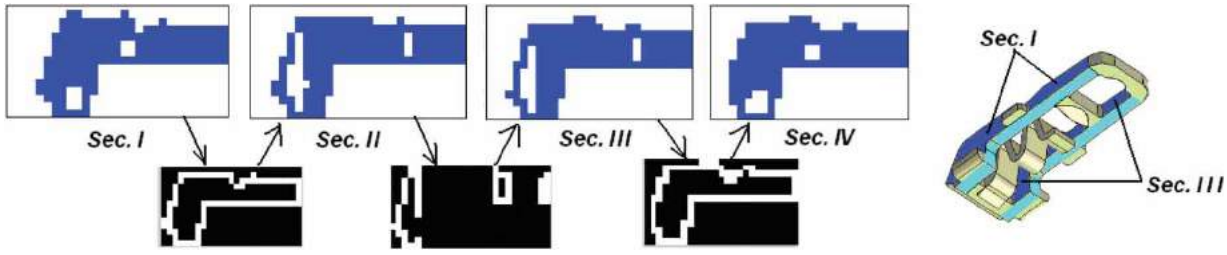

Fig. 8: Feature recognition: from selected boundary to protrusion definition. Binary images represent union of boundaries found in the sections between the investigated planes.

(ii) area of the filled region and (iii) number of closed area included in the bounding box. From this analysis it can be argued that the first and the second section (Sec. I and Sec. II of Fig. 8) are the starting and the ending planes of a protrusion, similarly to the third and the fourth section (Sec. III and Sec. IV of Fig. 8). On the contrary from Sec. II to Sec. III no specific volume derives (thus there is a pocket to be investigated starting from other reference directions). Fig. 8 describes this scheme in terms of image union of the boundaries found in the sections between the investigated planes. To better understand this conclusion the CAD model of the part is reported on the right part of Fig. 8 highlighting section I and III and related volumes found by the algorithm (in cyan).

With similar reasoning starting from the cyan and the yellow empty areas of the second and the third section of Fig. 7 another two protruded volumes can be found so that the two component's details in Fig. 9(a) are recognised (cyan and yellow details). Finally, from cyan and yellow areas of the first and fourth section of Fig. 7 compared with the binary images of the remaining four clusters that have been found normal to the y axis, the four protrusions depicted in magenta in Fig. 9(b) derive.

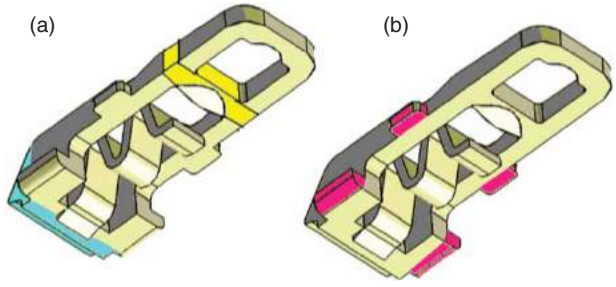

Fig. 9: Volume recognition associated to the remaining 4 clusters normal to *y* axis.

4. DISCUSSION

To run the proposed approach some assumptions are necessary. They mainly concern with the choice of the total number of voxels, *N*; the threshold on the variance of the point distance from the voxels' best fitting plane and the normal dot product threshold. A sensitivity analysis of these assumptions is relevant to understand the robustness and the general applicability of the proposed approach on electromechanical components, that are characterised by normal protrusions or box-shaped features, without free-form surfaces.

The number of voxels superimposed to the cloud of points is the first parameter to be calibrated. It influences the "resolution" of the proposed approach, that means its precision to recognise planes and volumes. If voxel discretisation becomes coarser many details may be lost, so that the effective planes of the component are not recognised. It is of amount importance in case of box-shaped components with small wall thicknesses, since $step_i$ of eq. (2.1) must be able to set at least two voxels around a wall thickness. Thus to generalise the procedure it must be said that the zoom factor, *r*, must be computed by means of

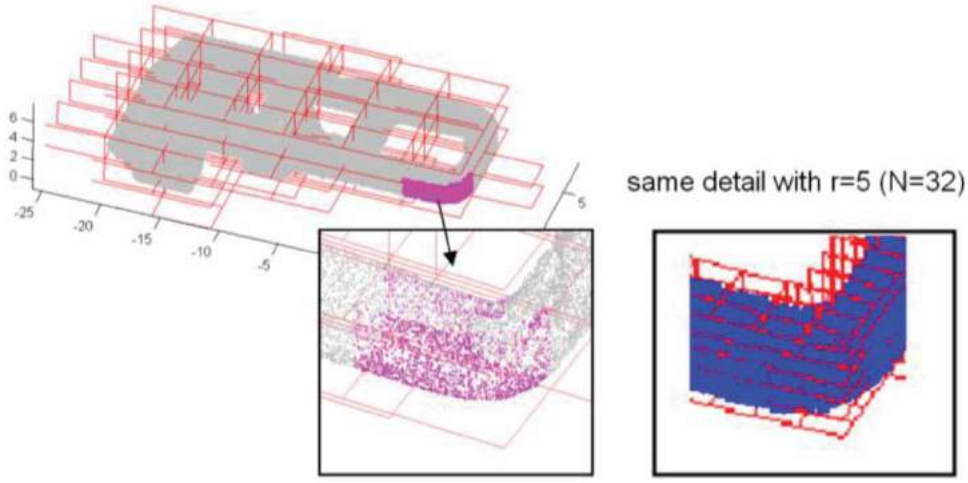

Fig. 10: Effect related to a reduction of the zoom factor, r.

eq. (2.1) and (2.2), setting $step_i$ as a function of the smallest significant length of the component. Fig. 10. shows a detail of the lost of resolution related to the adoption of $r = 3$ during the post-process of the din-rail clip. In this case a single voxel, like the one in the detail of Fig. 10, may contain a finite volume of the component, not only a surface region, so that the variance threshold will certainly exclude this part of the component, reducing the resolution of the approach. On the contrary in case of $r = 5$ the same area is subdivided into 6 voxels along z and 4 along y so that no voxels contain finite volumes of the component, and no risk of finite volume exclusion occurs.

According to eq. (2.1) and (2.2), the voxel discretisation is usually based on a base 2 numerical progression arresting the zoom factor r to 5 ($N = 32$). Fig. 11 shows a detail of a plane partition that has been achieved in case of a box-shaped component with small thickness. In this case $r = 5$ so that a $step_x$ equal to 1.14 mm is obtained. This value is less than the nominal thickness of the thinnest wall in that direction (1.65 mm) ensuring the recognition of both inner and outer surface.

Voxel density also impacts the computational efforts. Through them surface partition is made not on cloud mesh but on voxels' best fitting planes. Thus the computational cost of the partition, generally described as a function of the number of triangles [1], now becomes a function of the significant voxels. For the acquisition of the din-rail clip the number of triangles of the related tessellation file and the "true state" voxels are in a ratio of 11000/1896. Computation time of the voxel structure becomes now the bottleneck of the procedure, together with the region growing phase. Generally speaking this structure is an octree data structure that can take advantage of parallel computing or GPU programming. Overall, current implementation, that has been developed in MATLAB™ without any kind of parallelisation, is able to process 100 points/s on an Intel®Core™2Quad Processor@2.83GHz with 3.25GB of RAM.

Variance threshold has been inserted to distinguish voxel with curved or planar regions inside. Its value is found looking for the most populated bin of the occurrence histogram, that is also the one with the smallest value of variance. This assumption sounds to be consistent because the geometrical shapes of the investigated components have a large number of extended planar regions and both component manufacturing and acquisition are usually of good quality. Hence this means that small variances are expected for the most populated bins and the adoption of 10 or 20 bins (for zoom factor within 3 and 5) can be assumed as a robust solution.

The third relevant parameter is the normal dot product threshold. It is a threshold on a function of the L_2 orientation norm and it is applied during the clustering procedure to evaluate if: (i) the local best fitting plane associated to a generic V_{ijk} is parallel to the neighbouring ones; (ii) it is oriented as one of the reference axis, or in a more general case to the set of directions (a b c).

It works on the dot product of the directional cosines of two connected voxels and it may condition the clustering process since it is applied as a constraint of the region growing algorithm, searching for planes with a specific orientation. Fig. 12 shows the variation of the number of clusters that has been obtained changing threshold value in the range (0.50, 0.999) to search planes perpendicular to the three axes of the reference system (O, x, y, z). Fig. 12(a) is related to all the computed clusters for each reference direction. Fig. 12(b) considers only clusters with more than 4 voxels inside. Comparing these graphs it emerges that the cluster variations according to the threshold value are quite similar and some clusters made of less than 4 voxels are always present along each directions. Decreasing the

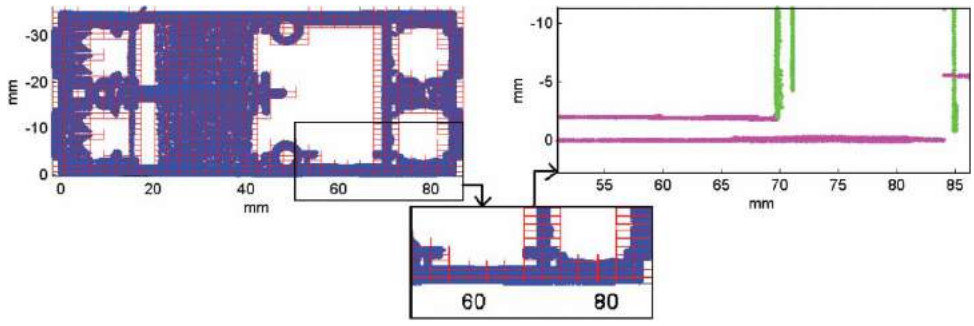

Fig. 11: Plane partition for a box-shaped component with small wall thickness ($r = 5$, $N = 32$).

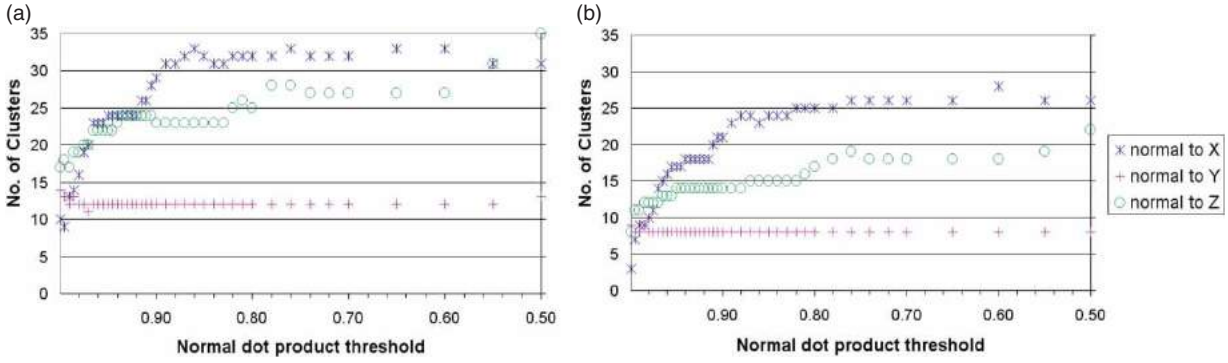

Fig. 12: Sensitivity analysis on the normal dot product threshold: (a) no. of clusters normal to reference axis; (b) no. of clusters normal to reference axis, excluding clusters made of less than 4 voxels.

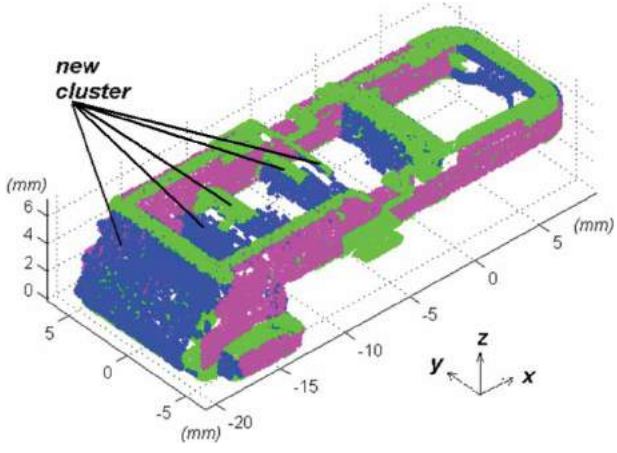

Fig. 13: New cluster found assuming a normal dot product greater or equals to 0.500.

threshold, obviously, also sloping planes are evaluated coherent with the reference axis, so the number of clusters increases with the angle allowed through the dot product threshold. The presence of clusters made with less than five voxels can be ascribed to voxels nearby curved surfaces (e.g. that ones at the centre of the din-rail clip) that, locally, can be well approximated by planes (each voxel represents a volume of $step_x$ x $step_y$ x $step_z$ that in this case is equal to $1.26 \times 0.74 \times 0.56\,\text{mm}^3$).

Fig. 13 shows the cluster result achieved with a dot product ≥ 0.500 highlighting the new sloping plane that are now included in the clusters normal to x. On the contrary in the case of planes perpendicular to the y axis the number of clusters does not change, as shown in Fig. 12, because the component has no sloping planes along this direction.

5. CONCLUSIONS

The paper proposes the first set-up of a procedure for point cloud segmentation and part type recognition based on a 3D discretisation methodology. It aims to simplify the reverse engineering post-processing of dense point clouds acquired for Computer Aided Tolerance Inspection of electromechanical components made by plastic injection moulding.

Thanks to a 3D discretisation, based on the introduction of a voxel matrix able to encompass and subdivide the point cloud, the surface regions found during the partition step can be associated to component volumes through the analysis of the morphological components of the binary image derived from the voxels attributes of each surface cluster ('true state' if points are included or 'false state' if they are not). This

analysis can be ascribable to volume feature recognition of the component according to a set of proper rules of classification that in this case have been defined and applied to recognise normal protrusions. By means of an industrial test case the proposed approach has been explained and preliminary tested. The processing is completely automatic without asking cloud tessellation or user interaction. Through the test case, planar surfaces normal to the reference axis of the component were recognised, then some of them were linked to their volume features to give a preliminary evidence about the recognition of component protrusions along one of the reference axes. As future development, combining this methodology with the information taken from the CAD model database of the component, a tolerance inspection without CAD model alignment will be developed.

Some considerations have also been pointed out about the assumptions made to set up the proposed approach. They concern with the density of the voxel discretization and the two thresholds for the surface partition, that is an hybrid region growing – hierarchical clustering procedure directly applied on the voxels. Voxel density impacts on precision and computational efforts. The total number of voxels must be set as a function of the smallest significant length of the component. Doing so it has been demonstrated that the proposed approach is able to investigate box-shaped components or with protusions, also with small thickness. These kinds of geometry describe electromechanical components exhaustively, since they do not have free-form surfaces. Concerning the computational efforts a benchmark with other well-established methods has been planned after the consolidation of the current implementation. At the moment it requires about 10^{-2} s/points and the most time consuming part of the procedure is related to the cluster merge and the voxels' structure creation. Both of them may be improved through parallel computing.

For components with protrusions robust thresholds were found. In particular for the variance distribution that is applied to distinguish voxels associated to small radii or non planar surfaces the adoption of the most populated bin of the occurrence histogram, that is also that one with the smallest value of variance, results consistent and non correlated with the variation of the number of bins (optimal solutions are in the range of [10, 20] bins for voxel matrices from $8 \times 8 \times 8$ to $32 \times 32 \times 32$). The second threshold is related to the normal dot product between pairs of planes of the connected voxels. It performs a region growing partitioning checking voxels plane towards specific orientations, as shown through the sensitivity analysis of Section 4. Decreasing the threshold, obviously, also planes different from the original set of significant directions are evaluated coherent with the clusters, so their number increases together with the angle allowed through the dot product threshold in accordance with a tolerance of about 6°-8° for each set of clusters.

REFERENCES

[1] Attene, M.; Falcidieno, B.; Spagnuolo, M.: Hierarchical mesh segmentation based on fitting primitives, The Visual Computer, 22(3), 2006, 181–193. http://dx.doi.org/10.1007/s00371-006-0375-x

[2] Campana, F.; Germani, M.: Datum identification for tolerances control on dense clouds of points, Computer-Aided Design and Applications, 5(1-4), 2008, 209–219. http://dx.doi.org/10.3722/cadaps.2008.209-219

[3] Di Stefano, P.; Bianconi, F.; Di Angelo, L.: An approach for feature semantics recognition in geometric models, Computer-Aided Design, 36(10), 2004, 993–1009. 10.1016/j.cad.2003.10.004

[4] Germani, M.; Mandorli, F.; Mengoni, F.; Raffaeli, R.: CAD-based environment to bridge the gap between product design and tolerance control, Precision Engineering, 34(1), 2010, 7–15. http://dx.doi.org/10.1016/j.precisioneng.2008.10.002

[5] Keller, P.; Bertram, M.; Hagen, H.: Reverse engineering with subdivision surfaces, Computing, 79(2-4), 2007, 119–129. http://dx.doi.org/10.1007/s00607-006-0191-1

[6] Lee, K. H.; Park, H.: Automated inspection planning of free-form shape parts by laser scanning, Robotics and Computer-Integrated Manufacturing, 16(4), 2000, 201–210. http://dx.doi.org/10.1016/S0736-5845(99)00060-5

[7] Prieto, F.; Redarce, T.; Lepage, R.; Boulanger, P.: An automated inspection system, Int. J. Adv. Manufact. Technol., 19, 2002, 917–925. http://dx.doi.org/10.1007/s001700200104

[8] Son, S.; Park, H.; Lee, K. H.: Automated laser scanning system for reverse engineering and inspection, International Journal of Machine Tools and Manufacture, 42(8), 2002, 889–897. http://dx.doi.org/10.1016/S0890-6955(02)00030-5

[9] Shamir A.: A survey on Mesh Segmentation Techniques, Computer Graphics Forum, 27(6), 2008, 1539–1556. http://dx.doi.org/10.1111/j.1467-8659.2007.01103.x

[10] Shen, J., Yoon, D.: Advances and prospects of digital metrology, Computer-Aided Design and Applications, 9(6), 2012, 825–835. http://dx.doi.org/10.3722/cadaps.2012.825-835

[11] Yadong Li; Peihua Gu: Free-form surface inspection techniques state of the art review, Computer-Aided Design, 36(13), 2004, 1395–1417, ISSN 0010-4485, http://dx.doi.org/10.1016/j.cad.2004.02.009